

# The legacy of the Pleistocene megafaunal extinctions on nutrient availability in Amazonia

## Table of contents

Overview	pg 2
Justification for the random walk	pg 3
Estimate of $D_{\text{excrement}}$ and $D_{\text{body}}$	pg 5
Consumption of nutrients	pg 6
Estimates of coefficients for $D$	pg 9
1D solution	pg 10
2D solution	pg 12
Continental scale analysis	pg 16
Possibilities to test predictions	pg 17
Tables	pg 19
Figures	pg 21
References	pg 24

17

## 18 Overview

19 In this paper, our goal is to estimate diffusive lateral nutrient fluxes by herbivores. In diffusion,  
20 the flux is proportional to the local concentration difference in material, with a constant of proportionality  
21 termed the “diffusivity”  $D$  (length<sup>2</sup>/time). The equation that best incorporates the diffusive properties of  
22 animals is the following reaction diffusion equation:

$$23 \quad \frac{dP}{dt} = D \frac{\partial^2 P}{\partial x^2} - KP + G \quad [1]$$

24 where  $K$  is a first order loss rate and  $G$  is a gain rate. To calculate a diffusion term we estimate  $D$  based  
25 on the random walk with the form:

$$26 \quad D = \frac{(\Delta x)^2}{2\Delta t} \quad [2]$$

27 Where  $\Delta x$  is a change in distance and  $\Delta t$  is a timestep of duration  $t$ . In general, a diffusivity can be  
28 derived from a random walk<sup>1-3</sup>. The “random walk” has been derived previously<sup>4</sup>.

29

30

31

## *Justification for the random walk*

Individual animals do not move randomly, but the net movement of all animals over long time periods (>1000 years) begins to approximate random motion. There is a large literature describing how different animal species overlap in space by consuming different foods and moving and sleeping in different patterns to avoid a variety of predators<sup>5-7</sup>. Internal demographics of animal groups will also change which will lead to shifting ranges and boundaries of the group over time<sup>8</sup>.

Next, large herbivores patterns will change in response to changing climate. For instance, herbivores often track landscape patterns in grass productivity<sup>9</sup> which will change in response to variable rainfall patterns<sup>10</sup>, which have experienced large global shifts over the past 15,000 years. Such interannual variation in climate alters the productivity of the landscape, which drives changes in animal foraging intensity<sup>11,12</sup>. These shifting patterns will serve to further move herbivore patterns from their current routes. For instance, in Kenya, during wet years there is a net nutrient input into certain patches because the impala dominate, but in dry years there may be a net loss, because the cattle dominate<sup>13</sup>. Due to these reasons, the net movement of all animals over long periods will approach an approximation of randomness.

As long as there is an underlying substrate concentration gradient, over long periods of time if the net movement is approximately random, animals will move the nutrients across the gradient. This seems to contradict literature showing that megafauna concentrate nutrients in small scale patches<sup>13</sup>. However, there is no contradiction, only a difference in the time, distance, and lack of a substrate concentration gradient. The study on megafaunal nutrient concentration focused on small nutrient patches in central Kenya (~1ha nutrient rich vegetation per 1km<sup>2</sup> nutrient poor vegetation) within homogenous nutrient poor metamorphic soil substrate. To the north of that study sites are rich basaltic soils of N. Kenya and Ethiopia. As these small patches of nutrient concentration shift across the landscape on decadal and larger timescales, nutrients will flow from the nutrient rich basalt to the nutrient poor metamorphic substrate

from patch to patch, through the large herbivores, over hundreds of km's and thousands of years. We have used our model to show a similar process for Kruger Park between nutrient rich basalts and granites in a companion paper<sup>14</sup>.

There is evidence that the small scale nutrient hotspots shown in the Augustine et al. 2003 paper will shift with time. That paper depicts the creation of nutrient hotspots by the corralling of cattle where significant quantities of dung accumulate over time<sup>13</sup>. They then measure a significant decline in the nutrients of these areas as they are abandoned over time. It is unlikely that these nutrients are lost but instead redistributed, thus showing how nutrient hotspots can build up but then move over short time periods (~40 years).

This process has also been experimentally demonstrated in a recent study where the authors measured the total seed biomass transported between the white water floodplains and the terra firme forests by a population of woolly monkeys. They show that a single, relatively small species can transport phosphorus in quantities similar to that arriving from atmospheric deposition<sup>15</sup>. There was no net movement of seed biomass between the two regions, but P was transported between the sites only due to the nutrient concentration gradient. There are several other similar studies showing the net movement of nutrients by animals<sup>16,17</sup>. Our mathematical framework enables us to estimate this process over all animals and long periods of time.

*Estimate of  $D_{\text{excreta}}$*

Nutrients can be moved by animals through either their dung or flesh. Nutrients moved in dung will have different distance and time scales than those moved in the flesh. We therefore calculate  $D$  for each separately. Below we start with  $D$  for dung.

$\Delta x$  is the daily displacement or day range (DD) of a single animal (DD; km), and  $\Delta t$  is a day. The length scale for diffusivity of ingestion and excretion is the day range multiplied by the average gut passage time (PT; fractions of a day). The time scale is again the food passage time (PT). Therefore, putting this in the framework of the random walk, we estimate that the diffusivity for transport of its dung is  $D_{\text{excreta}} \sim (DD \cdot PT)^2 / (2 \cdot PT)$ , where the numerator is in  $\text{km}^2$  and the denominator is in days.

*Estimate of  $D_{\text{body}}$*

Next, we calculate a  $D$  term for nutrients incorporated into the animal's body. The diffusivity for nutrients in an animal's bodymass,  $D_{\text{bones}}$ , is related to the lifetime of the animal  $L$  (days) and the residence time of these nutrients is  $L$ . The length scale is the home range (HR;  $\text{km}^2$ ). The mean displacement over the lifetime of an animal is related to the range length (RL) and approximately  $HR^{0.5}/2\pi$ . Therefore, if HR is the range used throughout an animal's lifetime, then  $D_{\text{body}} \sim RL^2/2L$  or  $HR/(8\pi^2L)$ , where the numerator is in  $\text{km}^2$  and the denominator is in days.

99

## 100 *Consumption of nutrients*

101           Next, we need to estimate the amount of food and nutrients consumed by a population of animals  
102 per area.  $P(x,t)$  is the mass (kg P km<sup>-2</sup>) of a nutrient. The mass of P at position  $x$  at time  $t+\Delta t$  is given by:

$$103 \quad P(x, t + \Delta t) = P(x, t) - \text{losses} + \text{gains} \quad [3]$$

104 The *losses* term is represented in Equation 3 by  $\alpha p(x,t)$ , the fraction of animals leaving  $x$  at time  $t$ . The  
105 loss of a nutrient in dry matter consumed and transported by a population of animals is

$$106 \quad \alpha \frac{\text{animals}}{\text{km}^2} \frac{\text{kgDM}/\Delta t}{\text{animal}} \frac{\text{kgP}}{\text{kgDM}} (x, t) \Delta t = \alpha \cdot PD \cdot MR \cdot [P](x, t) \Delta t = \alpha Q[P](x, t) \Delta t \quad [4]$$

107 The loss rate of P (kg DM km<sup>-2</sup>) is the population density of animals (PD; #/km<sup>2</sup>) consuming dry matter  
108 (DM) to fulfil their metabolic requirements (MR; kg DM/animal/day). The product of PD and MR is the  
109 population consumption rate of DM (denoted  $Q$  here), such that  $Q\Delta t$  is the mass of DM consumed in  $\Delta t$   
110 (kg DM km<sup>-2</sup>). The consumption of the nutrient itself is then determined by  $Q[P](x,t)$ , which has units kg  
111 P km<sup>-2</sup>, equivalent to  $P$ , the numerator on the left. Gains from adjacent regions will be represented as  
112  $Q[P](x+\Delta x, t)$  and  $Q[P](x-\Delta x, t)$ . A fraction  $\varepsilon$  of the consumed nutrient is incorporated into bodymass,  
113 while the rest  $(1-\varepsilon)$  is excreted.

114           We estimate  $\varepsilon$  as 22.4% for megafauna based on the gross food assimilation efficiency of  
115 elephants<sup>18</sup>. Incorporation of phosphorus into the body is, of course, more complicated with relative P  
116 fraction of biomass increasing with size due to the greater investment in bone growth in larger vertebrates  
117<sup>19</sup>. It also changes with animal age as full grown adult vertebrates need less P than immature growing  
118 animals. However, since we account for both the fraction in the biomass and the fraction excreted and  
119 there are no fates of the nutrient other than bodymass or excrement, we use the simple value of 22.4%.

120 To account for the large uncertainty in this term, in a sensitivity study we increase and decrease it by 0.1  
 121 (12.4% and 32.4%).

122 Consider the budget of just the fraction  $(1-\varepsilon)$  of consumed nutrient that will be excreted:

$$123 \quad P(x, t + \Delta t) = P(x, t) - (1 - \varepsilon) \left[ \alpha Q[P](x, t) + \frac{\alpha}{2} Q[P](x + \Delta x, t) + \frac{\alpha}{2} Q[P](x - \Delta x, t) \right] \quad [5]$$

124 By analogy to the derivation the random walk, we arrive at the equation:

$$125 \quad \frac{\partial P}{\partial t} = (1 - \varepsilon) Q D_{excreta} \frac{\partial^2 [P]}{\partial x^2} \quad [6]$$

126 Adding in the fraction of nutrient incorporated into bodymass we get the complete budget equation:

$$127 \quad \frac{\partial P}{\partial t} = (1 - \varepsilon) Q D_{excreta} \frac{\partial^2 [P]}{\partial x^2} + \varepsilon Q D_{body} \frac{\partial^2 [P]}{\partial x^2} \quad [7]$$

128 The state variable on the left and the right are not the same;  $P$  is per area and  $[P]$  is per kg DM. Let  $B$  be  
 129 total plant biomass (kg DM km<sup>-2</sup>) such that  $[P]B = P$ . We note that  $B$  has the same units as  $Q$ . Dividing  
 130 both sides by  $B$ :

$$131 \quad \frac{\partial [P]}{\partial t} = (1 - \varepsilon) \frac{Q}{B} D_{excreta} \frac{\partial^2 [P]}{\partial x^2} + \varepsilon \frac{Q}{B} D_{body} \frac{\partial^2 [P]}{\partial x^2} \quad [8]$$

132  $B$  represents total plant biomass but animal consumption is only from edible parts of that biomass.

133 Therefore  $B' = \alpha B$ , where  $\alpha$  is the edible fraction of total biomass. We assume for simplicity here that all  
 134  $P$  made available is taken up, on a fast timescale and used in edible parts. We may revisit this assumption  
 135 in future work. If these fractions can be assumed equal, then:

$$136 \quad \frac{\partial [P]}{\partial t} = (1 - \varepsilon) \frac{Q}{\alpha B} D_{excreta} \frac{\partial^2 [P]}{\partial x^2} + \varepsilon \frac{Q}{\alpha B} D_{body} \frac{\partial^2 [P]}{\partial x^2} \quad [9]$$

137 If  $Q/B$  can be assumed constant, then:

$$\frac{\partial P}{\partial t} = \Phi_{excreta} \frac{\partial^2 P}{\partial x^2} + \Phi_{body} \frac{\partial^2 P}{\partial x^2} \quad [10]$$

where the [P] terms on both sides have been multiplied by  $\alpha B$ , and

$$\Phi_{excreta} = (1 - \varepsilon) \frac{Q}{\alpha B} D = (1 - \varepsilon) \frac{PD}{\alpha B} * MR * \frac{(DD * PR)^2}{2 * PR} \quad [11]$$

$$\Phi_{body} = \varepsilon \frac{Q}{\alpha B} D = \varepsilon \frac{PD}{\alpha B} * MR * \frac{HR}{8\pi^2 L} \quad [12]$$

We solve the equations above using datasets and methods described in the next section.



#### Coefficients for $\Phi$ from data

We compiled data for as many herbivore species as we could find for weight, day range, home range, lifetime, population density, and metabolic rate. We used a common taxonomic authority<sup>20</sup>, available online at <http://www.bucknell.edu/msw3/export.asp>. We compiled data for terrestrial mammals at the species level ( $n = 5278$  unique taxa) but only used herbivores in our calculations. We collected data for longevity and metabolic rate from the AnAge database<sup>21</sup>; population density<sup>22</sup>; day range<sup>23</sup>; and home range<sup>24</sup>, which all include  $M$  as a predictor variable, as well as  $M$ <sup>25</sup>. We use the equation from<sup>26</sup> for food passage time. Each scaling term is not perfect but will approximate the “average” animal well which is important for our study because we incorporate all animals in the ecosystem. Certain terms, such as that for population density<sup>27</sup>, are also more controversial than others, but even population density shows a strong relationship with mass for large animals (although not for smaller animal).

We estimated  $\Phi$  as a function of  $M$  in two ways: first, we calculated the allometries for each term as a function of  $M$  (using ordinary least squares) and combined the resulting coefficients to yield an allometric equation for  $\Phi$  that results from scaling arguments (SOM Figure 1 and SOM Table 2). For example, to calculate the grey and black lines for  $QD_{\text{scaled}}$  in Figure 2a, we calculated the allometries for each attribute and combine them (SOM Figure 1 for herbivores  $>10\text{kg}$ ). Second, we multiplied the terms together to estimate  $\Phi$  directly, and fit the allometric equation using the data themselves (Figure 2a). In Figure 2, we were able to calculate  $QD_{\text{fit}}$  for the following fourteen species: *Eulemur fulvus*, *Propithecus verreauxi*, *Alouatta palliata*, *Cercopithecus mitis*, *Colobus guereza*, *Dipodomys merriami*, *Perognathus longimembris*, *Apodemus flavicollis*, *Apodemus sylvaticus*, *Rattus rattus*, *Capreolus capreolus*, *Odocoileus virginianus*, *Cervus elaphus*, *Kobus ellipsiprymnus*.

166

167 *1D solution*

168 Below is the solution for equation 1 in 1 dimension:

169 An ordinary differential equation for a nutrient with exogenous gains  $G$  ( $\text{kg P km}^{-2} \text{ day}^{-1}$ ) and first  
170 order losses  $K$  ( $\text{day}^{-1}$ ) has the following form:

$$171 \quad \frac{dP}{dt} = -KP + G \quad [13]$$

172 The steady state  $P_{ss}$  of this system is  $G/K$ . We then add the diffusion term  $\Phi$  which adds the potential for  
173 lateral fluxes to emerge from horizontal gradients in  $P$ :

$$174 \quad \frac{dP}{dt} = \Phi \frac{d^2P}{dx^2} - KP + G \quad [14]$$

175 We make the following two substitutions,  $u = KP - G$  and  $v = ue^{kt}$ , to get the homogeneous equation

$$176 \quad \frac{dv}{dt} = \Phi \frac{d^2v}{dx^2} \quad [15]$$

177 We assume a boundary condition with one edge ( $x=0$ ) with a fixed concentration of a nutrient that is  
178 continuously replenished. Crank<sup>28</sup> presented the following solution. Let a line source of material have  
179 concentration  $v_0$  within a domain of width  $d\xi$ , such that its initial mass is  $v_0 d\xi$ . The general solution for  
180 this line source, if diffusion is only in the  $+x$  direction, is

$$181 \quad v(\xi, t) = \frac{v_0 d\xi}{\sqrt{\pi Dt}} \exp\left(\frac{-\xi^2}{4\Phi t}\right) \quad [16]$$

182 Integrating this expression over  $d\xi$  yields:

$$183 \quad v(x, t) = \frac{v_0}{\sqrt{\pi \Phi t}} \int_x^\infty \exp\left(\frac{-\xi^2}{4\Phi t}\right) d\xi = v_0 \frac{2}{\sqrt{\pi}} \int_{x/\sqrt{4\Phi t}}^\infty \exp(-\eta^2) d\eta \quad [17]$$

184 where  $\eta = \xi/\sqrt{4\Phi t}$ . In evaluating the integral, consider the error function

$$185 \quad \text{erf}(z) = \frac{2}{\sqrt{\pi}} \int_0^z \exp(-\eta^2) d\eta \quad [18]$$

186 where  $\text{erf}(\infty) = 1$  and  $\text{erf}(0) = 0$ , and the error function complement  $\text{erfc}(z) = 1 - \text{erf}(z)$ . The integral then  
187 equals

$$188 \quad \frac{2}{\sqrt{\pi}} \int_{x/\sqrt{4\Phi t}}^{\infty} \exp(-\eta^2) d\eta = \frac{2}{\sqrt{\pi}} \int_0^{\infty} \exp(-\eta^2) d\eta - \frac{2}{\sqrt{\pi}} \int_0^{x/\sqrt{4\Phi t}} \exp(-\eta^2) d\eta \quad [19]$$

189 yielding the solution

$$190 \quad v(x, t) = v_o \text{erfc}\left(\frac{x}{\sqrt{4\Phi t}}\right) \quad [20]$$

191 By the previous substitutions,  $v_o = e^{kt}(KP_o - G)$ , where  $P_o$  is the nutrient concentration at the  $x=0$   
192 boundary. Backsubstituting  $P(x, t) = (v(x, t)e^{-kt} + G)/K$ , the solution in conventional units is:

$$193 \quad P(x, t) = \left(P_o - \frac{G}{K}\right) \text{erfc}\left(\frac{x}{\sqrt{4\Phi t}}\right) + \frac{G}{K} \quad [21]$$

194 We use equation 21 to calculate SOM figure 2. We estimate  $G$  as  $0.48 \text{ kg P km}^{-2} \text{ yr}^{-129}$ , and local  
195 weathering at  $2.5 \text{ kg P km}^{-2} \text{ yr}^{-1}$  (see below), for a  $G$  of  $2.98 \text{ kg P km}^{-2} \text{ yr}^{-1}$ ,  $K$  as  $0.00007 \text{ yr}^{-1 30}$ , and  $P_o$  as  
196  $600 \text{ kg km}^{-2}$  (SOM Table 2). These figures show the distribution over time from a starting point for  
197 current fauna of  $\Phi_{\text{excreta}} = 0.027 \text{ km}^2 \text{ yr}^{-1}$  (SOM figure 2 bottom) and then including the extinct megafauna  
198  $\Phi_{\text{excreta}} = 4.4 \text{ km}^2 \text{ yr}^{-1}$  (SOM figure 2 top).

199

200

201

202

## 2D solution

We could not solve equation 1 directly for a 2D scenario and we therefore use the Crank-Nicolson method to numerically solve equation 1 at each pixel at a time step of 10 years<sup>31</sup>. We estimate flooded white water pixels using a map of flooded areas from Hess et al. (2002) calculated using synthetic aperture radar at 30 meter resolution<sup>32</sup>. We then separate nutrient rich white water rivers (including the Ucayali, Marañon, Napo, Caqueta, and Madeira) from nutrient poor black and clear water rivers according to figure 1 in McClain et al. (2008)<sup>33</sup>. We estimate that vegetation growing in the whitewater floodplain have an average leaf P concentration of  $1.50 \text{ mg g}^{-1}$  which is continuously replenished ( $600 \text{ kg P km}^{-2}$  assuming an average LAI of 4, and a SLA of  $100 \text{ g m}^{-2}$ ) (SI Table 1)<sup>34</sup>. We assume an efficient transfer of the phosphorus from the herbivore dung to the edible biota because nutrients, especially P, recycle rapidly and efficiently in tropical forests<sup>35</sup>.

We estimate the spatial distribution of dust into the Amazon basin based on figure 8a from Mahowald et al. 2005<sup>29</sup>. In a sensitivity study we double and halve these numbers due to uncertainty on how these numbers may have varied in the past (i.e. such as due to changes in the jet stream). We estimate soil moisture in the Amazon basin showing a gradual drying from the northwest to the southeast and soil moisture changing from  $0.6$  to  $0.5 \text{ m}^3 \text{ m}^{-3}$  along this gradient. We map higher P concentrations in the more fertile western region following Higgins et al. (2011) figure 3 top<sup>36</sup>. This increased fertility is probably related to the removal of cation-poor surface sediments through river movement which exposes cation-rich sediments from the Pebas formation<sup>36</sup>. We estimate that vegetation in this region has a continually replenished source of  $300 \text{ kg P km}^{-2}$ . There is very little data on average local weathering rates in the central and eastern Amazon. However, the ratio of P carried by whitewater rivers to the more numerous black and clear water rivers is  $806 \text{ Mg P}$  versus  $43 \text{ Mg P}$ . The area of black and clear water rivers are  $\sim 3$  times greater than white water rivers<sup>33</sup> and the P from black and clear water rivers is from local weathering, dust, and herbivore input. Therefore, we roughly assume the highly weathered Eastern

lowland soils have a local weathering rate of  $\sim 2.5 \text{ kg P km}^{-2}$ , which we double and halve in a sensitivity study<sup>37</sup>. In addition, if we assume the long term steady state P (G/K) equals the labile P pool, with a median value of  $\sim 50 \text{ Mg km}^{-2}$  in the Eastern Amazon (see below)<sup>38</sup>, a loss rate of  $0.00007 \text{ yr}^{-1}$  (see below)<sup>30</sup>, and average dust input of  $0.48 \text{ kg km}^{-2} \text{ yr}^{-1}$ <sup>29</sup>, then to achieve steady state, there must be an additional  $\sim 2.5 \text{ kg P km}^{-2}$  which we attribute to local weathering.

We estimate P losses from the system based on the following equations from Buendia et al. 2010<sup>30</sup>:

$$LQ(s) = k_l s^c \quad [22]$$

$$L_o = k_r * LQ(s) * P_o \quad [23]$$

$$L_d = LQ(s) * \frac{P_d}{n * Zr * s} \quad [24]$$

Where  $s$  is yearly averaged soil moisture (dimensionless),  $c$  is 3,  $k_l$  is runoff or leakage at saturation which is  $0.1 \text{ (yr}^{-1}\text{)}$ ,  $k_r$  is the losses regulation rate  $0.002 \text{ (yr}^{-1}\text{)}$ ,  $P_o$  is organic P,  $P_d$  is the dissolved P,  $Zr$  is soil depth (1m),  $n$  is soil porosity (0.4),  $L_o$  is the loss rate of  $P_o$  and  $L_d$  is the loss rate of  $P_d$ . Equation 9 in Buendia et al. 2010 includes a  $k_f$  term or a loss rate from ice, wind, humans, or fire which we do not include because we assume these to be minimal in the Amazon forest prior to the widespread arrival of modern humans. We estimate the steady state ratios of  $P_o$  to  $P_d$  following figure 2 in Buendia et al. 2010. We estimate the average total loss rate for the Amazon Basin is  $0.00007 \text{ yr}^{-1}$ . Buendia et al. 2010 calculates a steady state  $L_d$  for the Amazon basin of  $\sim 3.5 \text{ kg km}^{-2} \text{ yr}^{-1}$  and  $L_o$  of  $\sim 7 \text{ kg km}^{-2} \text{ yr}^{-1}$ . Our loss rates have a similar ratio of  $\sim 2 L_o = L_d$ . This is an important, yet highly uncertain part of our results and therefore as part of a sensitivity study we double and halve the loss rate. Loss rates of P through occlusion of P are an order of magnitude smaller than loss rates of organic and dissolved P (figure 7 in Buendia et al. 2010) and any uncertainty in occlusion rates will be incorporated within the large range of our sensitivity study.

We estimate the mass of both extinct and extant South American fauna from the Pleistocene and the Holocene based on data from Smith et al.2003 (N=904)<sup>25</sup>. At present it is unknown which extinct megafauna would have lived in the Amazon forest. However, based on limited evidence we are able to make two lists, one of those with animals that “probably” would have ranges that would encompass the current Amazon basin, and one “possibly” could have inhabited the Amazon basin. Based on stable isotope evidence of C3 plant consumption and the location of fossil evidence, we assume that the following species inhabited forest areas of the Amazon: *Eremotherium* (3500kg) assume 1 of 2 species), *Haplomastodon* (6000kg), *Cuvieronius* (5000kg) assume 1 of 2 species, *Toxodon* (1100) assume 1 of 4 species, *Neochoeus* (1500kg) assume 1 of 2 species and *Tayassuidae* (1100kg) assume 1 of 3 species<sup>39,40</sup>. Based on a more liberal reading of the evidence, we assume the following species could also have dwelled in the Amazon: *Equus santaelenae*, *Glossotherium*, *Holmesina* (Personal communication E. Lindsey and A. Barnosky). Based on the QD equation of  $0.05 \cdot M^{1.17}$ , we calculate a QD value for the Amazon basin of  $2.4 \text{ km}^2 \text{ yr}^{-1}$  for the “probable” group and  $6.5 \text{ km}^2 \text{ yr}^{-1}$  for the “possible” group including all species from the “probable” group. In our simulations, we use the midrange value of  $4.4 \text{ km}^2 \text{ yr}^{-1}$ , and use 2.4 and  $6.5 \text{ km}^2 \text{ yr}^{-1}$  in the sensitivity study. We assume that each of these extinct forest megafauna had a distribution of 100% of the basin based on the abundance of megafauna fossil remains throughout South America and widely dispersed large seeded fruits<sup>41,42</sup>.

We display our current estimates of vegetation P with total P and labile P from Quesada et al. 2010 fig 2b<sup>38</sup> (SOM Figure 3). We convert this to  $\text{Mg km}^{-2}$  for each site using soil bulk density and soil depth provided in the supplementary material (S1 C.A. Quesada) of the paper. We also include data from Fyllas et al. 2009 for leaf P concentrations which we show as vegetation P ( $\text{Mg km}^{-2}$ ) with the assumption of a uniform SLA of  $100 \text{ g m}^{-2}$  and an LAI of 4<sup>35</sup>. Where the plots overlap (N=49), we calculate the ratio of vegetation P to labile P and use this to estimate % dust P going into vegetation. Parent material and soil evolutionary stage controls long term (geologic) total P concentrations<sup>38</sup>. Our model does not incorporate these properties and will not replicate current total soil P patterns and concentrations. Instead,

our simulations more closely replicate vegetation and labile P patterns because the megafauna increase the readily available form of P that is quickly taken up by the vegetation.

We assume a steady state in the absence of animal herbivory of  $G/K$  ( $\sim 50 \text{ Mg km}^{-2}$ ), where G is dust plus local weathering ( $0.48 \text{ kg P km}^{-2} \text{ yr}^{-1}$  plus  $\sim 2.5 \text{ kg P km}^{-2} \text{ yr}^{-1}$ ) and K is  $0.00007 \text{ yr}^{-1}$ . We estimate a median labile P of  $54 \text{ Mg km}^{-2} \text{ P}$  (SOM Figure 3b) in the Eastern Amazon from Quesada et al. 2010 and a median vegetation P of  $0.4 \text{ Mg km}^{-2} \text{ P}$  (SOM Figure 3c) from Fyllas et al. (2009). We are interested in the dust P that will enter the vegetation pool, which we estimate as  $\sim 1\%$  based on the fact that vegetation P is  $\sim 1\%$  of labile P (SOM Figure 3a), and therefore, we apply a multiplication of 0.01 to our dust term.

*Continental estimates of D*

We used the IUCN spatial database on mammal species and their ranges<sup>43</sup> to develop a gridded, global estimate of QD for modern animals<sup>14</sup>. We used this gridded estimate to calculate QD for modern species for continental estimates of Table 1 and for the Amazon basin for Figure 3. We assigned the mean value for the genera or family to species with no body mass data. Edible biomass at 1° resolution was estimated using foliar NPP from the CASA carbon cycle model<sup>44</sup>.

For extinct species, we use the database from Smith et al. 2003<sup>25</sup>. Since the ranges of individual species are not currently accurately known, we estimate that at a continental scale each species has a range of ~8% of the continent<sup>45</sup>. We estimate the exact range for each species in the same way as Barnosky (2008) with Africa (8.6%), Australia (7.8%), North America (8.2%), South America (7.2%), and Eurasia (8.1%). This is a highly uncertain term, so we add and subtract 30%, which is incorporated into our uncertainty shown in table 1. There was no data for certain extinct species in Smith et al. 2003 for Eurasia and these values were obtained from Barnosky (2008). We assume the percentage of the continent covered in ice during the Pleistocene as: N. America (50%), Eurasia (10%), and S. America (5%)<sup>45</sup>.



306

307 *Possibilities to test predictions*

308         We recognise that we do not yet present any direct evidence that nutrient availability across the  
309 Amazonia has declined since the megafaunal extinctions. Instead we have put forward a quantified  
310 testable model based on available ecological and geophysical evidence. The collection of direct evidence  
311 of nutrient decline following megafaunal loss would require a substantial experimental campaign, and  
312 here we propose several potential ways to test our predictions from this study. We would predict a  
313 greater quantity of phosphorous flowing out the mouth of the Amazon today than during the era when  
314 megafauna still were present in the Amazon basin. We can analyse ocean sediment data from the Ocean  
315 Drilling Program (ODP) (<http://www-odp.tamu.edu/database/>) near the Amazon Fan for changing  
316 phosphorous and other nutrient concentrations in a manner similar to which has been done for pollen and  
317 isotopes<sup>46</sup>.

318         We can look for changes in nutrient concentrations across a nutrient concentration gradient in the  
319 presence and exclusion of megafauna. Certain parts of Kruger Park have had all animals >5kg excluded  
320 from large regions of the park for 37-43 years and the park has a nutrient concentration gradient due to  
321 the granite/basalt substrate. We can compare nutrient gradients both where the animals have been  
322 excluded and where they still exist. We predict a diffusion of nutrients across the granite/basalt gradient  
323 in the regions with the megafauna, but more of a step change nutrient concentrations in the part of the  
324 park without megafauna. This can be tested through airborne analysis of exclusion experiments in Kruger  
325 National parks<sup>47</sup>.

326         For longer time-scale tests we could compare the sharpness of changes in ecosystem P content  
327 (plants, litter and labile soil pools) across sharp geomorphological boundaries (e.g. floodplains vs  
328 adjoining terraces), in regions with and without megafauna. In the absence of significant lateral diffusion,  
329 ecosystem labile P content should show a step-change across the boundary, reflecting the sharp change in

330 base substrate. With increasing lateral diffusion, this step change in ecosystem P content becomes  
331 increasingly blurred, and the degree of blurring is a direct measure of the diffusivity parameter in our  
332 equation. We predict that the measured “blurring” will be much greater in megafauna-rich regions of  
333 Africa than in the equivalent geomorphological transitions in Amazonia.

334       Finally, we can directly test our theory by measuring nutrient concentrations near fertilized farms  
335 and forests that are regularly raided by megafauna such as elephants (or experimentally fertilize these  
336 areas). We can find out when fertilization of the farm began and how often and by which animals it is  
337 raided. From this, we would predict a nutrient gradient into the forest from the fertilized farm. We can  
338 test the dung piles as well as the vegetation in the area to determine if the rate of nutrient spread matches  
339 that of our predictions.

340

341 **SI Table 1** – Average P concentrations for leaves, wood, bark, and fruits from Terra firme and blackwater  
 342 forests and whitewater flood plain forests based on data from Furch and Klinge 1989 (leaves, wood and  
 343 bark) and Stevenson and Guzman-Caro 2010 (fruit) in units of  $\text{mg g}^{-1}$  <sup>15,34</sup> (N= number of tree species  
 344 analysed).

	Leaves $\text{mg g}^{-1}$	Wood $\text{mg g}^{-1}$	Bark $\text{mg g}^{-1}$	Fruit $\text{mg g}^{-1}$
Whitewater flood plain	1.50 (N=88)	0.59 (N=60)	0.80 (N=42)	2.2 (N=10)
Terra Firme and blackwater forests	0.55 (N=220)	0.13 (N=246)	0.16 (N=22)	1.6 (N=13)
Difference	0.95	0.46	0.64	0.4

345

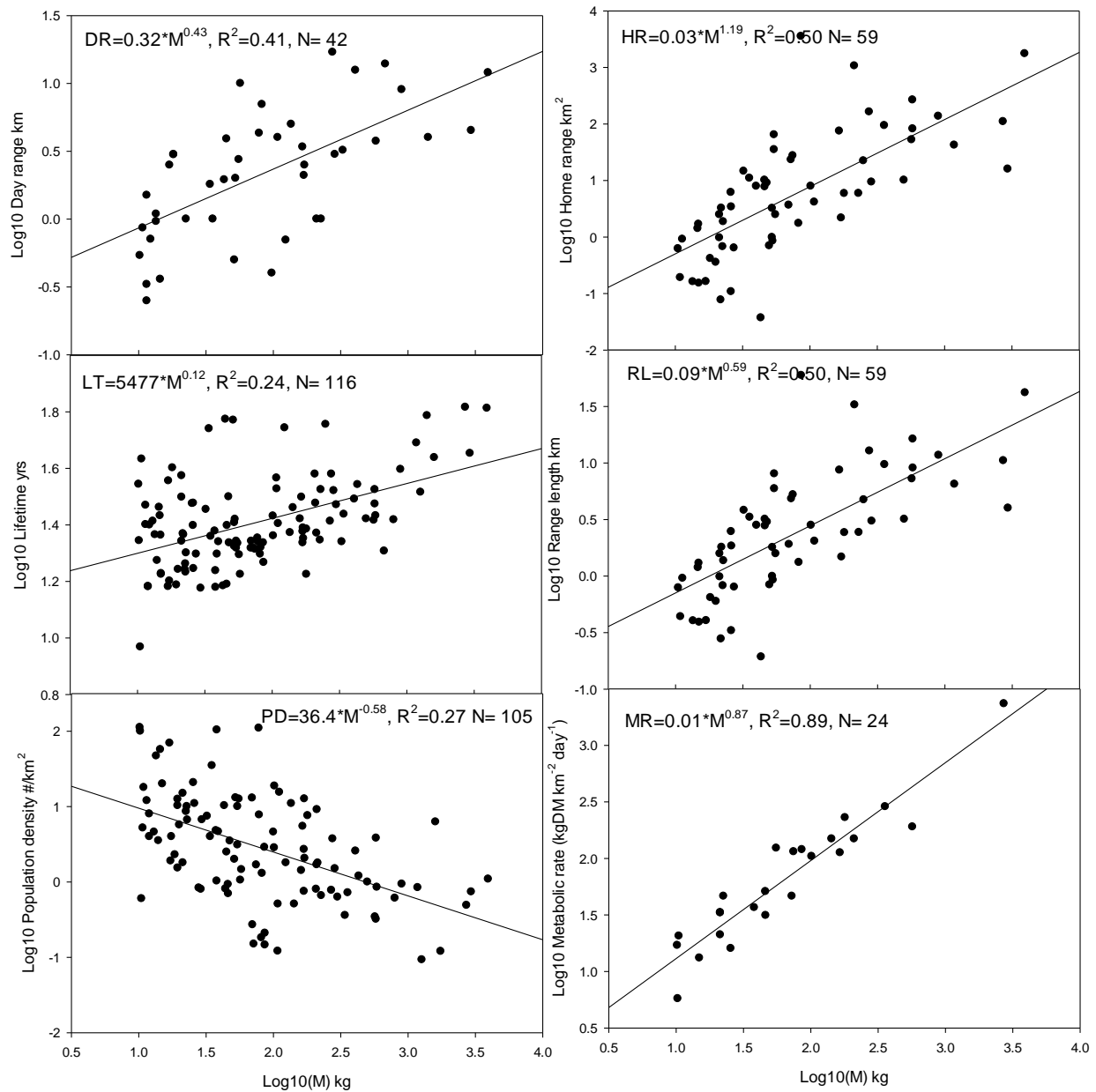
346

347

348 **SI Table 2** - Table 1. Allometric fits for herbivores >10kg. For the fecal diffusivity fit equation we use  
 349 all herbivores to increase the sample size.

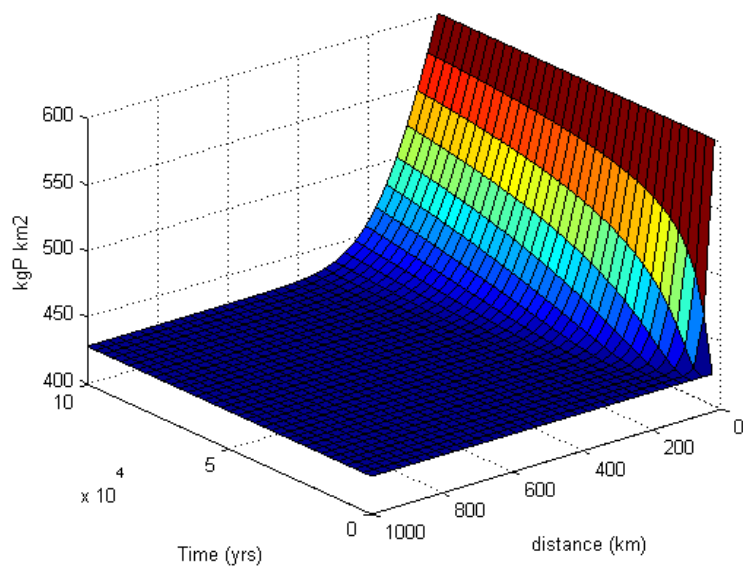
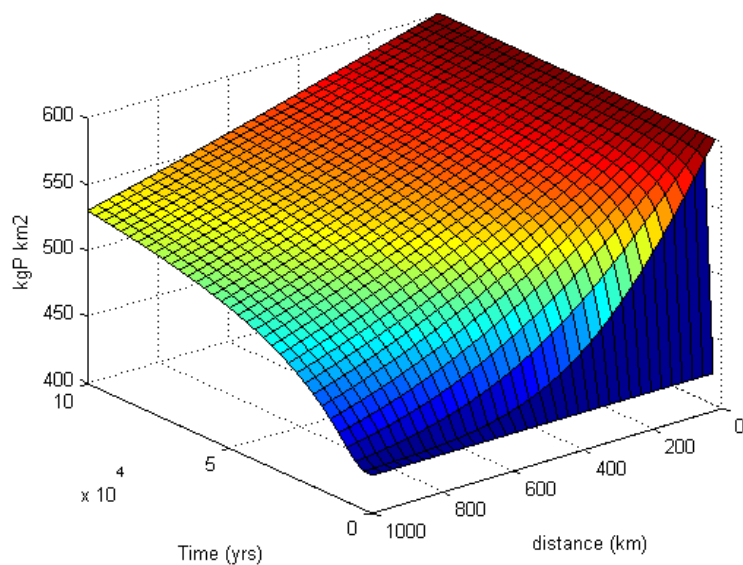
Dependent Variable	Units	Equation	N	r <sup>2</sup>
Population Density	#/km <sup>2</sup>	$36.35 * M^{-0.58}$	105	0.27
Metabolic Demand	kgDM/#/day	$0.01 * M^{0.87}$	24	0.89
Mature Longevity	Days	$5477 * M^{0.12}$	116	0.24
Day Range	Km	$0.32 * M^{0.43}$	42	0.41
Home Range	km <sup>2</sup>	$0.03 * M^{1.19}$	59	0.50
Range Length ( $\sqrt{HR}$ )	Km	$0.09 * M^{0.59}$	59	0.50
Passage rate*	Days	$0.29 * M^{0.28}$	-	-
Fecal Diffusivity, scaling herbivores >10kg	(kgDM/km <sup>2</sup> ) *(km <sup>2</sup> /day)	$0.0065 * M^{1.41}$	-	-
Fecal Diffusivity, fit all herbivores	(kgDM/km <sup>2</sup> ) *(km <sup>2</sup> /day)	$0.05 * M^{1.17}$	14	0.67
Bodymass Diffusivity, scaling herbivores >10kg	(kgDM/km <sup>2</sup> ) *(km <sup>2</sup> /day)	$6.5 * 10^{-7} * M^{1.35}$	-	-

350 \*equation from Demment and Van Soest et al. 1985 assuming a digestibility of 0.5<sup>26</sup>



352

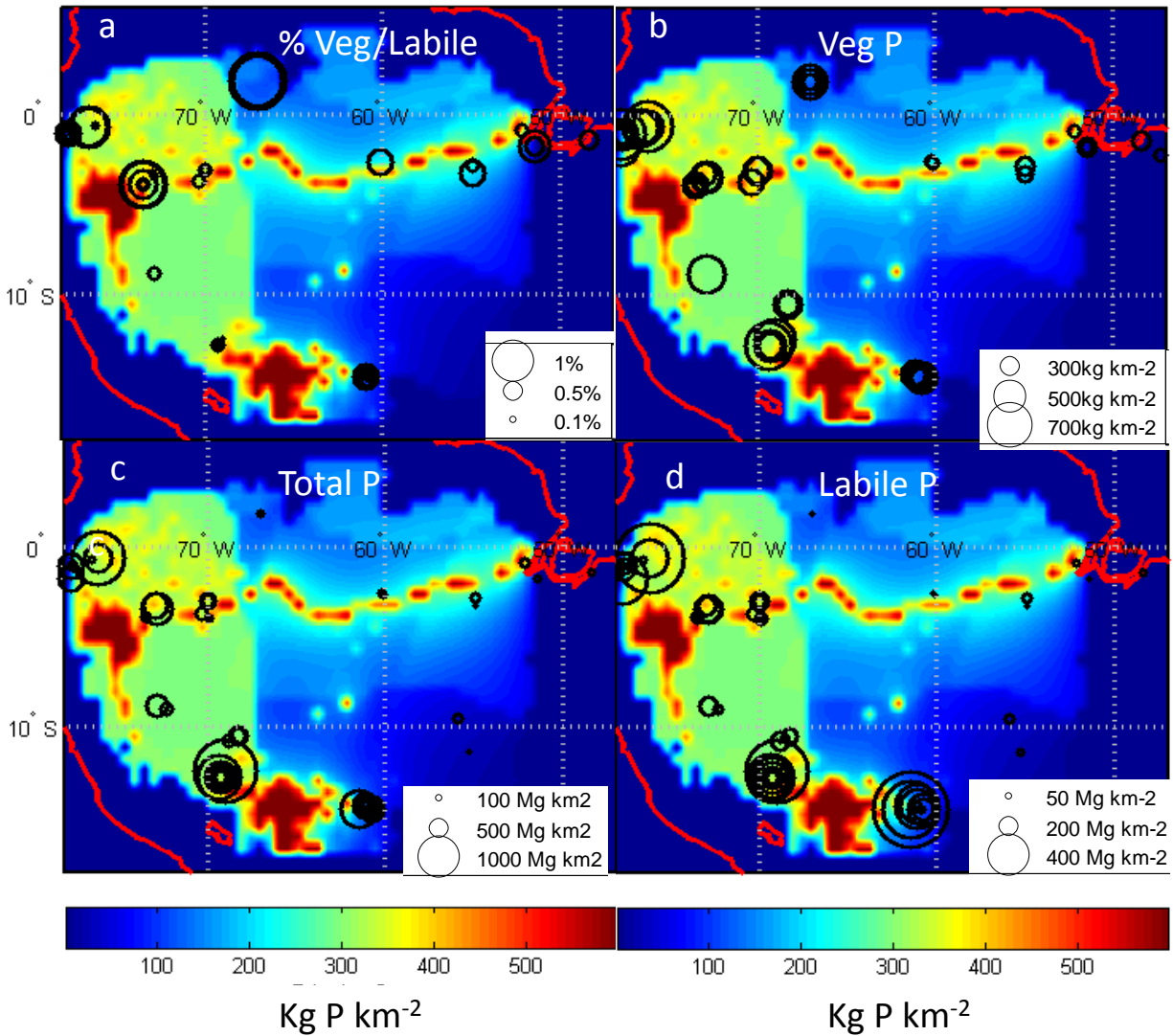
353 **SOM Figure 1** –  $\text{Log}_{10}$  mass versus  $\text{log}_{10}$  transformed values of day range (km) (top left), home range  
 354 ( $\text{km}^2$ ) (top right), lifetime (yrs) (middle right), range length (the square root of home range) (km) (middle  
 355 left), population density (number of individuals per  $\text{km}^2$ ) (bottom left), and metabolic rate (kg DM  $\text{km}^{-2}$   
 356 day $^{-1}$ ) (bottom right) for herbivores >10kg.



358

359 **SOM Figure 2** – (top) Lateral distribution of nutrients starting from initial conditions over a 1000km  
 360 distance from a nutrient supply (e.g. the Amazon floodplain) and a 100,000 year period with a  $\Phi_{\text{excreta}}$   
 361 value of  $4.4 \text{ km}^2 \text{ yr}^{-1}$  (representing lateral diffusion by modern and extinct fauna), (bottom) a  $\Phi_{\text{excreta}}$  value  
 362 of  $0.027 \text{ km}^2 \text{ yr}^{-1}$  (representing lateral diffusion by modern fauna only).

363



**SOM Figure 3** – A comparison of our modelled modern-day phosphorus estimates (kg P km<sup>-2</sup>) (same as Figure 3b) in the background and estimates of (a) percent vegetation/ labile P, (b) vegetation P (kg km<sup>-2</sup> from Fyllas et al. 2009<sup>35</sup>, assuming a SLA of 100g m<sup>-2</sup> and an LAI of 4), (c) total P (Mg km<sup>-2</sup>), and (d) labile P (Mg km<sup>-2</sup>) measured in the Amazon basin from Quesada et al. 2010<sup>38</sup>.

371

## 372 References

- 373 1 Okubo, A. & Levin, S. A. *Diffusion and ecological problems : modern perspectives*. 2nd edn,  
374 (Springer, 2001).
- 375 2 Ovaskainen, O. & Crone, E. E. in *Spatial Ecology Chapman & Hall/CRC Mathematical &*  
376 *Computational Biology* 63-83 (Chapman and Hall/CRC, 2009).
- 377 3 Skellam, J. G. Random Dispersal in Theoretical Populations. *Biometrika* **38**, 196-218 (1951).
- 378 4 Berg, H. C. *Random Walks in Biology.*, (1993).
- 379 5 Ilse, L. M. & Hellgren, E. C. Resource Partitioning in Sympatric Populations of Collared Peccaries  
380 and Feral Hogs in Southern Texas. *J Mammal* **76**, 784-799, doi:Doi 10.2307/1382747 (1995).
- 381 6 Augustine, D. J. & McNaughton, S. J. Ungulate effects on the functional species composition of  
382 plant communities: Herbivore selectivity and plant tolerance. *J Wildlife Manage* **62**, 1165-1183,  
383 doi:Doi 10.2307/3801981 (1998).
- 384 7 Mcnaughton, S. J. Mineral-Nutrition and Spatial Concentrations of African Ungulates. *Nature* **334**,  
385 343-345, doi:Doi 10.1038/334343a0 (1988).
- 386 8 White, K. A. J., Lewis, M. A. & Murray, J. D. A model for wolf-pack territory formation and  
387 maintenance. *J Theor Biol* **178**, 29-43 (1996).
- 388 9 Frank, D. A., McNaughton, S. J. & Tracy, B. F. The ecology of the Earth's grazing ecosystems.  
389 *Bioscience* **48**, 513-521, doi:Doi 10.2307/1313313 (1998).
- 390 10 Ellis, J. E. & Swift, D. M. Stability of African Pastoral Ecosystems - Alternate Paradigms and  
391 Implications for Development. *J Range Manage* **41**, 450-459, doi:Doi 10.2307/3899515 (1988).
- 392 11 Boone, R. B., Coughenour, M. B., Galvin, K. A. & Ellis, J. E. Addressing management questions for  
393 Ngorongoro Conservation Area, Tanzania, using the SAVANNA modelling system. *Afr J Ecol* **40**,  
394 138-150 (2002).
- 395 12 Bailey, D. W. *et al.* Mechanisms that result in large herbivore grazing distribution patterns. *J*  
396 *Range Manage* **49**, 386-400 (1996).
- 397 13 Augustine, D. J., McNaughton, S. J. & Frank, D. A. Feedbacks between soil nutrients and large  
398 herbivores in a managed savanna ecosystem. *Ecological Applications* **13**, 1325-1337, doi:Doi  
399 10.1890/02-5283 (2003).
- 400 14 Wolf, A., Doughty, C.E., Malhi, Y. Lateral diffusion of nutrients by herbivores in terrestrial  
401 ecosystems. *Plos one* (2013).
- 402 15 Stevenson, P. R. & Guzman-Caro, D. C. Nutrient Transport Within and Between Habitats Through  
403 Seed Dispersal Processes by Woolly Monkeys in North-Western Amazonia. *American Journal of*  
404 *Primatology* **72**, 992-1003, doi:Doi 10.1002/Ajp.20852 (2010).
- 405 16 Frank, D. A., Inouye, R. S., Huntly, N., Minshall, G. W. & Anderson, J. E. The Biogeochemistry of a  
406 North-Temperate Grassland with Native Ungulates - Nitrogen Dynamics in Yellowstone-  
407 National-Park. *Biogeochemistry* **26**, 163-188 (1994).
- 408 17 Abbas, F., J. Merlet, N. Morellet, H. Verheyden, A. J. M. Hewison, B. Cargnelutti, J. M. Angibault,  
409 D. Picot, J. L. Rames, B. Lourtet, S. Aulagnier, and T. Daufresne. . Roe deer may markedly alter  
410 forest nitrogen and phosphorus budgets across Europe. *Oikos* (2012).
- 411 18 Rees, P. A. Gross Assimilation Efficiency and Food Passage Time in the African Elephant. *African*  
412 *Journal of Ecology* **20**, 193-198 (1982).
- 413 19 Elser, J. J., Dobberfuhl, D.R., MacKay, N.A., Schampel, J.H. Organism Size , Life History, and N:P  
414 Stoichiometry. Toward a unified view of cellular and ecosystem processes. *BioScience* **46** (1996).



- 415 20 Wilson, D. E. & Reeder, D. M. *Mammal species of the world : a taxonomic and geographic*  
416 *reference*. 3rd edn, (Johns Hopkins University Press, 2005).
- 417 21 de Magalhaes, J. P. & Costa, J. A database of vertebrate longevity records and their relation to  
418 other life-history traits. *J Evolution Biol* **22**, 1770-1774, doi:DOI 10.1111/j.1420-  
419 9101.2009.01783.x (2009).
- 420 22 Damuth, J. Interspecific Allometry of Population-Density in Mammals and Other Animals - the  
421 Independence of Body-Mass and Population Energy-Use. *Biol J Linn Soc* **31**, 193-246 (1987).
- 422 23 Carbone, C., Cowlshaw, G., Isaac, N. J. B. & Rowcliffe, J. M. How far do animals go?  
423 Determinants of day range in mammals. *American Naturalist* **165**, 290-297 (2005).
- 424 24 Kelt, D. A. & Van Vuren, D. H. The ecology and macroecology of mammalian home range area.  
425 *American Naturalist* **157**, 637-645 (2001).
- 426 25 Smith, F. A. *et al.* Body mass of late quaternary mammals. *Ecology* **84**, 3403-3403 (2003).
- 427 26 Demment, M. W. & Van Soest, P. J. A Nutritional Explanation for Body-Size Patterns of Ruminant  
428 and Nonruminant Herbivores. *American Naturalist* **125**, 641-672 (1985).
- 429 27 Hayward, A., Kolasa, J. & Stone, J. R. The scale-dependence of population density-body mass  
430 allometry: Statistical artefact or biological mechanism? *Ecological Complexity* **7**, 115-124,  
431 doi:DOI 10.1016/j.ecocom.2009.08.005 (2010).
- 432 28 Crank, J. *The mathematics of diffusion*. 2d edn, (Clarendon Press, 1975).
- 433 29 Mahowald, N. M. *et al.* Impacts of biomass burning emissions and land use change on  
434 Amazonian atmospheric phosphorus cycling and deposition. *Global Biogeochemical Cycles* **19**, -,  
435 doi:Artn Gb4030 Doi 10.1029/2005gb002541 (2005).
- 436 30 Buendia, C., Kleidon, A. & Porporato, A. The role of tectonic uplift, climate, and vegetation in the  
437 long-term terrestrial phosphorous cycle. *Biogeosciences* **7**, 2025-2038, doi:DOI 10.5194/bg-7-  
438 2025-2010 (2010).
- 439 31 Crank, J. & Nicolson, P. A Practical Method for Numerical Evaluation of Solutions of Partial  
440 Differential Equations of the Heat-Conduction Type. *Proceedings of the Cambridge Philosophical*  
441 *Society* **43**, 50-67 (1947).
- 442 32 Hess, L. L., Melack, J. M., Novo, E. M. L. M., Barbosa, C. C. F. & Gastil, M. Dual-season mapping of  
443 wetland inundation and vegetation for the central Amazon basin. *Remote Sensing of*  
444 *Environment* **87**, 404-428, doi:DOI 10.1016/j.rse.2003.04.001 (2003).
- 445 33 McClain, M. E. & Naiman, R. J. Andean influences on the biogeochemistry and ecology of the  
446 Amazon River. *Bioscience* **58**, 325-338, doi:Doi 10.1641/B580408 (2008).
- 447 34 Furch, K., Klinge, H. Chemical relationships between vegetation, soil and water in contrasting  
448 inundation areas of Amazonia. *SPEC. PUBL. BR. ECOL. SOC.* , 189-204. (1989.).
- 449 35 Fyllas, N. M. *et al.* Basin-wide variations in foliar properties of Amazonian forest: phylogeny,  
450 soils and climate. *Biogeosciences* **6**, 2677-2708 (2009).
- 451 36 Higgins, M. A. *et al.* Geological control of floristic composition in Amazonian forests. *Journal of*  
452 *Biogeography* **38**, 2136-2149, doi:DOI 10.1111/j.1365-2699.2011.02585.x (2011).
- 453 37 Richey, J. E. & Victoria, R. L. in *Interactions of C, N, P, and S Biogeochemical Cycles and Global*  
454 *Change*. (ed Mackenzie FT Wollast R, Chou L) 123-140 (Springer, 1993).
- 455 38 Quesada, C. A. *et al.* Variations in chemical and physical properties of Amazon forest soils in  
456 relation to their genesis. *Biogeosciences* **7**, 1515-1541, doi:DOI 10.5194/bg-7-1515-2010 (2010).
- 457 39 MacFadden, B. J. Diet and habitat of toxodont megaherbivores (Mammalia, Notoungulata) from  
458 the late Quaternary of South and Central America. *Quaternary Res* **64**, 113-124, doi:DOI  
459 10.1016/j.yqres.2005.05.003 (2005).

- 40 Sanchez, B., Prado, J. L. & Alberdi, M. T. Feeding ecology, dispersal, and extinction of south  
American pleistocene gomphotheres (Gomphotheriidae, Proboscidea). *Paleobiology* **30**, 146-161  
(2004).
- 41 Janzen, D. H. & Martin, P. S. Neotropical Anachronisms - the Fruits the Gomphotheres Ate.  
*Science* **215**, 19-27 (1982).
- 42 Do Nascimento, W. M. O., De Carvalho, J. E. U. & Muller, C. H. Occurrence and geographical  
distribution of bacuri. *Revista Brasileira De Fruticultura* **29**, 657-660 (2007).
- 43 IUCN. (2010).
- 44 Field, C. B., Behrenfeld, M. J., Randerson, J. T. & Falkowski, P. Primary production of the  
biosphere: Integrating terrestrial and oceanic components. *Science* **281**, 237-240 (1998).
- 45 Barnosky, A. D. Megafauna biomass tradeoff as a driver of Quaternary and future extinctions.  
*Proceedings of the National Academy of Sciences of the United States of America* **105**, 11543-  
11548, doi:DOI 10.1073/pnas.0801918105 (2008).
- 46 Maslin, M. A., Ettwein, V. J., Boot, C. S., Bendle, J. & Pancost, R. D. Amazon Fan biomarker  
evidence against the Pleistocene rainforest refuge hypothesis? *Journal of Quaternary Science* **27**,  
451-460, doi:Doi 10.1002/Jqs.1567 (2012).
- 47 Asner, G. P. & Levick, S. R. Landscape-scale effects of herbivores on treefall in African savannas.  
*Ecology Letters* **15**, 1211-1217, doi:DOI 10.1111/j.1461-0248.2012.01842.x (2012).